SIFT DESK

Journal of Chemical Engineering And Bioanalytical Chemistry(ISSN:2575-5641)

Cybotactic Effect on Nitrogen and Phosphorus Hyperfine Coupling Constants in β -Phosphorylated Nitroxides.

DOI: 10.25177/JCEBC.2.1.3

Research

Author: Sylvain R. A. Marque

January 2018

Received Date: 03rd Dec 2017
Accepted Date: 18th Dec 2017
Published Date:05th Jan 2018

Gerard Audran,[*a] Jean-Patrick Joly,[a] Sylvain R. A. Marque[*a,b]

[a] Aix Marseille Univ, CNRS, ICR, UMR 7273, case 551, Avenue Escadrille Normandie-Niemen, 13397 Marseille Cedex 20 France.
[b] N. N. Vorozhtsov Novosibirsk Institute of Organic Chemistry SB RAS, Pr. Lavrentjeva 9, 630090 Novosibirsk, Russia.
E-mail: g.audran@univ-amu.fr, sylvain.marque@univ-amu.fr

CORRESPONDENCE AUTHOR

Sylvain R. A. Marque
Email: sylvain.marque@univ-amu.fr

CONFLICTS OF INTEREST

There are no conflicts of interest for any of the authors.

Abstract:

Solvent effect is investigated on β-phophorylated nitroxides carrying electron widthdrawing groups exhibiting various steric hindrances. Solvent effect on nitrogen and phosphorus hyperfine coupling constants highlights the entanglement of polar and steric effects on the changes in hyperfine coupling constants.

Introduction

Nitroxyl radicals are currently applied as probe in several fields as Site Directed Spin-Labeling to investigate dynamics of protein, as spin probes in Materials Sciences and in Medecine.[] Recently, we highlighted the interest to use β-phosphorylated nitroxides as spin label,[] as imaging agent[] and as spin probe.[] Such applications of nitroxides rely on changes in both the nitrogen and phosphorus hyperfine coupling constants a_N and a_P, respectively, depending on their surrounding.[] We showed that changes in a_N and a_P are dramatically dependent on the structure of the nitroxyl radical.[,,,-] However, in the series of nitroxyl radical **3** only minor steric changes were investigated with **3a** and **3b,c**.[8,9] Indeed, one methyl group in **3a** is replaced either by the CH_2OAc (**3b**) or by the CH_2OPiv (**3c**). Hereafter, we report on the effect on a_N and a_P of more significant changes in the steric strain as Me group in **3a** is replaced by COOMe group in **3d** (Figure 1).

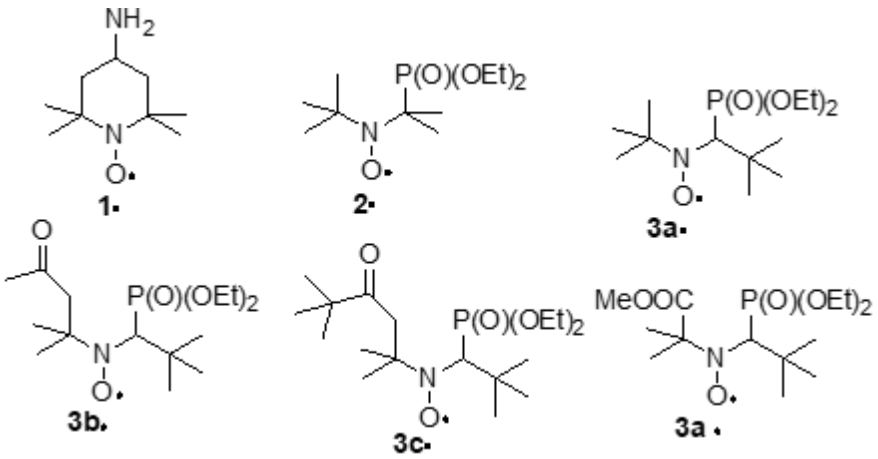

Figure 1. Nitroxides discussed in the article

Results and Discussion

Nitroxide **3d•** was prepared as already reported[] and the corresponding nitrogen and phosphorous hyperfine coupling constant (hcc) an and a_P, respectively, were measured as previously described.[6-11] Due to the presence of both *N*- and *P*-atoms at the positions a and b to the odd electron with nuclear spin $I_N = 1$ and $I_P = ½$, respectively, EPR signal of **2•**, **3a-d•** displays 6 lines (doublet of triplet) with a large doublet due to a_P and a small triplet due to a_N (Table 1).

Table 1. Nitrogen and phosphorus hyperfine coupling constants a_N and a_P[a] in various solvents for nitroxides 1•,2•, and 3a-d•

entry	solvent[b]	**1•**[c]	**2•**[d]		**3a•**[e]		**3b•**[e]		**3c•**[e]		**3d•**		
		a_N	a_N	a_P	a_N	a_P	a_N	a_P	a_N	a_P	a_N	a_P	E_T^N
1	pentane	15.15	14.06	41.35	13.54	46.19	13.61	45.67	13.43	55.07	13.59	43.19	0.009
2	*n*-hexane	15.22	14.30	41.68	-[g]	-[g]	13.49	45.55	13.43	54.97	13.76	43.02	0.009
3	CHex	15.19	14.23	40.68	13.54	46.10	13.49	45.42	13.43	55.17	13.76	42.84	0.006
4	octane	15.22	14.56	41.35	13.50	46.20	13.49	45.55	13.54	55.17	13.41	43.02	0.012
5	benzene	15.53	14.56	35.32	13.74	45.14	13.61	44.68	13.54	55.75	13.58	42.15	0.111
6	toluene	15.46	14.73	36.63	-[g]	-[g]	13.61	44.8	13.54	55.55	13.76	42.50	0.099
7	*t*-BuPh	15.47	14.56	38.33	13.70	45.70	13.49	45.05	13.54	55.55	13.59	42.84	0.099
8	PhBr	15.57	14.56	32.64	-[g]	-[g]	13.74	44.18	13.66	56.03	13.59	41.97	0.182

9	pyridine	15.66	14.90	31.00	13.86	44.49	13.61	43.69	13.89	56.32	13.76	41.45	0.302
10	AcPh	15.64	14.73	31.64	-[g]	-[g]	13.61	44.06	13.66	56.26	13.76	41.80	0.306
11	*t*-BuPH/CH_2Cl_2	15.61	14.73	37.50	13.90	44.70	13.74	43.94	13.68	56.32	13.76	41.80	-[g]
12	CH_2Cl_2	15.77	15.06	27.28	13.90	44.61	13.74	43.69	13.74	56.80	13.93	41.80	0.309
13	DCE	15.71	15.06	28.62	13.90	45.10	13.74	43.69	13.77	56.61	13.76	41.63	0.327
14	$CHCl_3$	15.77	15.23	27.95	13.98	45.46	13.86	44.67	13.77	57.09	13.76	42.67	0.259
15	CCl_4	15.40	14.56	37.50	-[g]	-[g]	13.61	45.55	13.54	55.75	13.58	43.19	0.052
16	DME	15.265	14.39	35.49	-[g]	-[g]	13.61	44.69	13.54	55.55	13.58	42.50	0.231
17	Et_2O	15.241	14.23	37.83	-[g]	-[g]	13.49	45.17	13.54	55.26	13.58	42.85	0.117
18	*i*-Pr_2O	15.23	14.23	39.50	13.62	45.82	13.61	45.30	13.54	54.97	13.76	43.02	0.105
19	*n*-Bu_2O	15.36	14.39	37.66	13.50	46.00	13.49	45.30	13.54	55.36	13.58	42.85	0.071
20	Me*t*-BuO	15.32	14.06	38.17	13.62	45.74	13.61	45.17	13.54	55.17	13.41	42.67	0.124
21	14D	15.45	15.06	31.64	13.78	45.31	13.61	44.55	13.66	56.13	13.58	42.32	0.164
22	THF	15.47	14.73	35.49	13.70	45.59	13.61	44.68	13.66	55.55	13.58	42.49	0.207
23	AcOEt	15.60	14.90	36.32	13.66	45.66	13.61	44.93	13.54	55.84	13.76	42.67	0.228
24	acetone	15.62	14.56	33.65	13.82	45.42	13.74	44.55	13.77	56.03	13.58	42.32	0.355
25	ACN	15.76	15.06	28.62	13.86	44.73	13.74	43.81	13.77	56.42	13.76	41.63	0.460
26	$MeNO_2$	15.86	15.06	26.78	13.94	44.45	13.86	43.56	13.89	56.90	13.76	41.45	0.481
27	DMSO	15.77	15.06	30.80	13.8	45.40	14.73	43.69	13.77	56.32	13.76	41.80	0.444
28	F	16.20	15.56	20.59	14.4	43.70	14.11	42.2	14.24	58.44	14.11	40.76	0.775
29	NMF	15.77	15.40	20.50	14.1	44.20	13.99	42.7	14.00	57.29	13.93	40.76	0.722
30	DMF	15.67	14.90	32.31	13.9	45.50	13.74	44.31	13.77	56.23	13.76	41.97	0.386
31	MeOH	16.20	15.56	20.75	14.1	45.70	13.86	43.94	13.89	58.06	13.93	41.97	0.762
32	EtOH	16.08	15.23	22.76	14	45.80	13.74	44.31	13.86	57.48	13.76	42.32	0.654
33	TFE	16.78	15.90	20.42	14.7	46.30	14.36	44.43	14.24	59.78	14.11	42.50	0.898
34	*i*-PrOH	16.04	15.23	25.44	13.94	45.94	13.74	44.68	13.77	57.19	13.76	42.50	0.546
35	*n*-BuOH	16.04	15.22	23.42	-[g]	-[g]	13.74	44.43	13.77	57.29	13.76	42.32	0.586
36	*t*-BuOH	15.91	15.06	29.96	13.9	46.50	13.74	45.17	13.54	57.09	13.76	42.84	0.389
37	BnOH	16.29	15.40	23.60	-[g]	-[g]	13.86	44.06	13.89	58.15	13.76	41.97	0.608
38	EG	16.30	15.40	21.59	13.74	45.54	14.11	43.91	14.12	58.53	14.11	41.80	0.790
39	TEG	15.30	15.23	21.76	13.62	45.42	13.99	44.43	13.89	57.48	13.76	41.97	0.682
40	water/MeOH	16.72	15.90	22.60	14.5	45.70	14.23	43.81	14.35	59.5	14.11	41.97	0.710
41	water	16.99	16.90	22.15	14.9	45.60	14.73	43.69	14.7	60.85	14.28	42.15	1.000
42	buffer[h]	-[g]	16.23	22.09	-[g]	-[g]	-[g]	-[g]	-[g]	60.85	14.28	42.15	-[g]
43	AcOH	16.19	-[g]	-[g]	-[g]	-[g]	13.86	44.93	13.77	58.54	13.76	42.67	0.648
44	Et_3N	15.32	15.06	39.5	13.58	46.10	13.61	45.42	13.54	55.35	13.41	42.84	0.043
45	*i*-Pr_2NH	-[g]	14.73	39.17	13.62	45.91	13.49	45.3	13.66	55.36	-[g]	-[g]	0.145

[a] a_N and a_P given in G. [b] CHex: *cyclo*hexane, *t*-BuPh: *tert*-butylbenzene, PhBr: bromobenzene, AcPh: acetophenone, DCE: 1,2-dichloroethane, DME: 1,2-dimethoxyethane, 14D: 1,4-dioxane, THF: tetrahydrofurane, AcOEt: ethyl acetate, ACN: acetonitrile, DMSO: dimethylsulfoxide, F: formamide, NMF: *N*-methylformamide, DMF: *N,N*-dimethylformamide, TFE: 2,2,2-trifluoroethanol, EG: ethylene glycol, TEG: triethylene glycol, AcOH: acetic acid, *i*-PenOH: *iso*-pentanol, Mecyc: methylcyclopentane, PhCl: chlorobenzene. [c] Given refs. [6,7]. [d] Given in ref. [8]. [e] Given ref. [11]. [f] Given in ref. [17,18]. [g] Not available. [h] Phosphate buffer NaH_2PO_4/Na_2HPO_4, 0.05 M, pH = 7.3

Hcc at position a is directly related to the spin population localized on the nucleus,[] and to the shape of the SOMO (Fermi contact term Q_N, eq. 1).[13] For p-radicals, the SOMO is of the *p* type and thus any increase in the *s* character leads to an increase in the spin population and, hence, to an increase in a_N.

$$a_X = cte \cdot Q_N \qquad \textbf{(1)}$$

For nitroxides, a decrease in a_N is observed for both a decrease in Q_N – because form **A** is favoured over zwiterionic form **B**[,,] (Figure 2) due to the presence of electron widthdrawing groups (EWG) – and a change in the hybridization (pyramidalization) at the nitrogen atom, varying from sp^3 to sp^2 (Figure 3), i.e., the higher the pyramidalization (form **C**), the higher the *s* character of the SOMO, and conversely.

The dramatic increase in polarity – electrical Hammet constant s_L are -0.06, 0.27, 0.28, 0.48, 0.48, and 0.61 – of the substitutents in the nitroxides **1•**, **2•**, **3a-d•** do not account for the decrease in a_N as expected (see *y*-intercept in Figure 4) by disfavouring mesomeric form **B** over form **A** (Figure 2). Indeed, a_N decrease from **1•** to **3a•** as expected but does not change significantly for **3a-d•**. This means that the effect of strong EWG attached to the nitroxyl moiety is balanced by a stronger pyramidalization at the *N*-atom in **3d•** than in **3b,c•** and **3a•** (Figure 3). Taking into account the large difference in s_L, the very similar slope for the plot a_N vs $E_T^{N[,]}$ for **1•** and **2•** denotes a better accessibility of the nitroxyl moiety in **2•** as in **1•** as more polar the nitroxide is, less sensitive a_N (slope in Figure 4) is to the effect of solvent. Taking into account the similar values of s_L for **3a•** and for **2•**, the smaller slope for **3a•** denotes a larger steric hindrance than in **2•** and then a lesser accessibility to the nitroxyl moiety. The smaller slopes for **3b-d•** than for **3a•** is ascribed to the higher polarity in **3b-d•** than in **3a•** and, hence, a lower sensitivity to the solvent effect. The smaller slope for **3d•** is ascribed to both higher polarity and likely higher steric hindrance around the nitroxyl moiety.

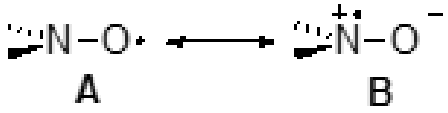

Figure 2. Mesomeric forms of the nitroxyl moiety

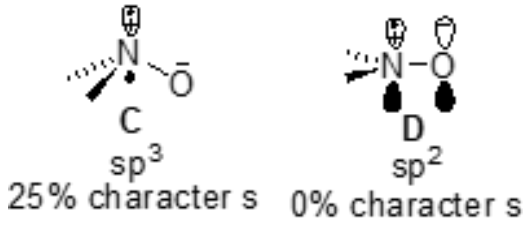

Figure 3. Canonical forms for the hybridization at the nitrogen atom of the nitroxyl moiety and % of *s* character of the SOMO

The Heller-Mconnel relationship (Scheme 1 and eq. (2))[] shows that a_P depends on the square of the cosine of the dihedral angle *q*. The Heller-McConnel relationship (2) shows – provided that there are no or only minor changes in the hybridization or in the mode of solvation – an increase in a_P as the spin population r_N^P increases when a_N increases.[13] The smaller *y*-intercept for **2•** than for **3a-d•** (Figure 5) is ascribed to a larger angle *q* meaning that the conformation are very different between **2•** and **3a-d•**. The very similar *y*-intercepts for **3a-d•** and its decreasing trends form **3a•** to **3d•** agrees with very close conformation and an increase in polarity decreasing the spin density r_N^P on the *N*-atom. The very similar and negative slopes for **3a-d•** denote same conformational changes which are much less important than in **2•** (Figure 5). Hence, the bond rotations N—CP are strongly restricted in **3a-d•**. The smaller changes in slope for **3a-d•** are not discussed are they are due to entangled polar and steric effects.

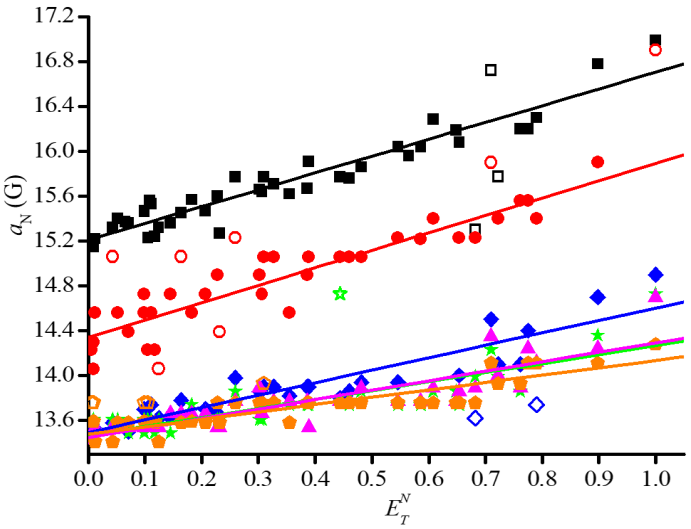

Figure 4. Correlations E_T^N vs a_N for **1•** (■), **2•** (), **3a•** (¿), **3b•**(ê), **3c•** (▲), and **3d•** (À). Empty symbols are for outliers

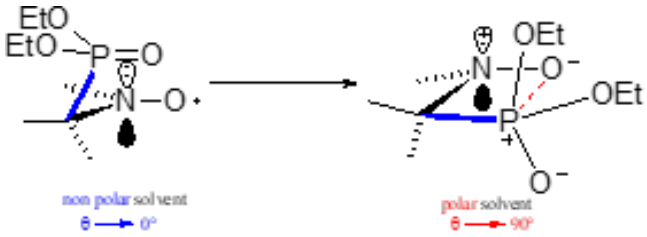

Scheme 1. Conformation change by rotation around the C—N bond from a non polar solvent to a polar solvent. Dotted line for the dipole-dipole interaction +•N—O^-••••$^+$P—O^-.

$$a_P = B_0 \cdot \rho_N^\pi + B_1 \cdot \rho_N^\pi \cdot \cos^2\theta \qquad \textbf{(2)}$$

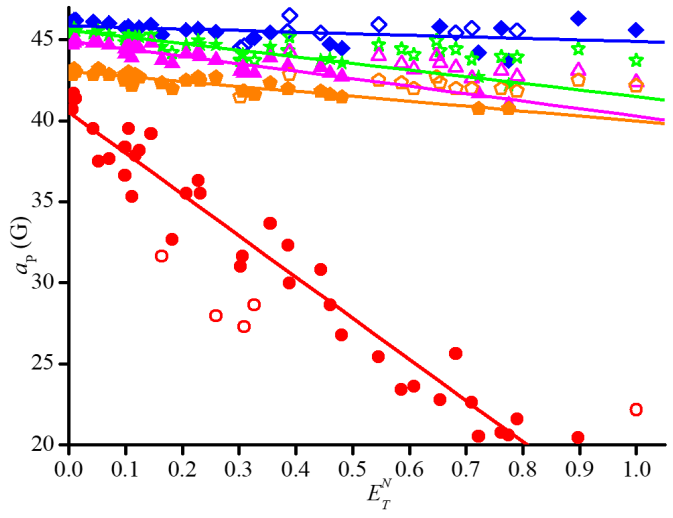

Figure 5. Correlations E_T^N vs a_P for **2•** (), **3a•** (¿), **3b•**(ê), **3c•** (▲), and **3d•** (À). Empty symbols are for outliers.

In recent articles,[6-11] we showed that the impact of conformational changes on a_P is probed using the dihedral angle q between the C—P bond and the $SOMO_{p*}$ on the N-atom of the nitroxyl moiety, as given in eq. (2). The value of $r_N^P B_1$ is solvent dependent and is known in non polar solvents for nitroxides carrying a diethoxyphosphonyl group,[19] and commonly accepted as $r_N^P B_1$ = 59 G in *n*-hexane or other similar non polar solvents. As r_N^P is proportional to a_N, the ratio $a_{P,n\text{-hexane}}/a_{P,n}$ (eq. 3) affords the value of q for each solvent and, hence, an insight into the solvent dependence of the conformation.

$$\frac{a_{P,n\text{-hexane}}}{a_{P,n}} = \frac{a_{N,n\text{-hexane}}}{a_{N,n}} \cdot \frac{\cos^2\theta_{n\text{-hexane}}}{\cos^2\theta_n} \qquad \textbf{(3)}$$

All nitroxides display (Figure 6) a decrease of a_P with increasing q meaning that all nitroxides experience the same solvent effect except at different extents as highlighted by Dq = 24° for **2•** and Dq = 6° for **3a-d•**. Although steric hindrance and polarity are very different in **3a-d•**, the relative mobility is the same but much lower than for **2•**. Moreover, the quasi-linear and decreasing distribution of a_P vs q denote that the conformational changes are overmatch the changes in polarity of the nitroxyl moiety and that these changes are quasi-monotonic with the solvent.

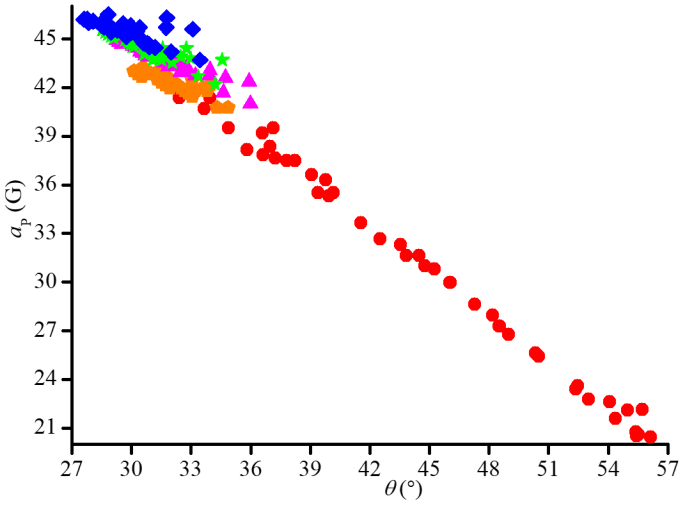

Figure 6. Plot q vs a_P for **2•** (), **3a•** (¿), **3b•**(ê), **3c•** (▲), and **3d•** (À). Empty symbols are for outliers.

CONCLUSION

As already observed and discussed for **2•** and **3a-c•**, changes in a_N and a_P with solvent polarity in **3d•** are governed by the interaction N+•—O$^-$····P+—O$^-$ between nitroxyl and phosphoryl moieties. Plots E_T^N vs a_N E_T^N vs a_P show that the changes in polarity and bulkiness of the substituents in **3d•** compared to **3a-c•** are baleanced by changes in hybridization at the *N*-atom and in conformations.

COMPETING INTEREST

The authors declare that they have no competing interests.

ACKNOWLEDGEMENTS

The authors thank Aix-Marseille University and CNRS for financial support. ANR was granted for funding this project (ANR-14-CE16-0023-01) managed by the French National Research Agency (ANR). SRAM thanks the Russian Science Foundation (grant 15-13-20020) for supporting the correlation analysis of this work. The authors thank RENARD network for the EPR platform.

REFERENCES

1. Likhtenshtein, G.; Yamauchi, J.; Nakatsuji, S.; Smirnov, A. I.; Tamura, R., *Nitroxides: Applications in Chemistry, Biomedicine, and Materials Science*, Wiley-VCH, 2008, and references therein.
2. Le Breton, N.; Martinho, M.; Kabitaev, K.; Topin, J.; Mileo, E.; Blocquel, D.; Habchi, J.; Longhi, S.; Rockenbauer, A.; Golebiowski, J.; Guigliarelli, B.; Marque, S. R. A.; Belle, V. *PhysChemChemPhys* **2014**, *16*, 4202-4209.
3. Audran, G.; Bosco, L.; Brémond, P.; Franconi, J.-M.; Koonjoo, N.; Marque, S. R. A.; Massot, P.; Mellet, P.; Parzy, E.; Thiaudière E., *Angew. Chem. Int. Ed.* **2015**, *54*, 45, 13379-13384.
4. Audran, G.; Bosco, L.; Brémond, P.; Butscher, T.; Marque, S. R. A. *Org. Biomol. Chem.* **2016**, *14,* 1228-1292.
5. *Stable Radicals: Fundamentals and Applied Aspects of Odd-Electron Compounds;* Hicks, R., Ed., Wiley, Hoboken, 2010, 173–229, and references therein.
6. Audran, G.; Bosco, L.; Brémond, P.; Butscher, T.; Franconi, J.-M.; Kabitaev, K.; Marque, S. R. A.; Mellet, P.; Parzy, E.; Santelli, M.; Thiaudière, E.; Viel, S. *RSC Advances* **2016**, *6*, 5653-5670.
7. Audran, G.; Bosco, L.; Brémond, P.; Butscher, T.; Marque S. R. A. *Appl. Magnet. Reson.* **2015**, *45*, 12, 1333-1342.
8. Audran, G.; Brémond, P.; Marque, S. R. A.; Obame, G. *ChemPhysChem* **2012**, *13*, 15, 3542-3548.
9. Audran, G.; Bosco, L.; Nkolo, P.; Bikanga, R.; Brémond, P.; Butscher, T.; Marque, S. R. A. *Org. Biomol. Chem.* **2016**, *14*, 3729-3743.
10. Bosco, L.; Butscher, T.; Marque, S. R. A. *Appl. Magn. Reson.* **2017***, 48, 4,* 379-406.
11. Nkolo, P.; Audran, G.; Brémond, P.; Bikanga, R.; Marque, S. R. A.; Roubaud, V. *Tetrahedron* **2017**, *73*, 3188-3201.
12. Audran, G.; Brémond, P.; Marque, S. R. A.; Yamasaki, T. *J. Org. Chem.* **2016**, *81,* 1981-1988.
13. Gerson, F.; Huber, W. *Electron Spin Resonance Spectroscopy of Organic Radicals*; Wiley-VCH, Weinheim, 2003.
14. Karoui, H.; Le Moigne, F.; Ouari, O.; Tordo, P. *Stable Radicals: Fundamentals and Applied Aspects of Odd-Electron Compounds*, Hicks, R., Ed., John Wiley & Sons, **2010**, pp. 173–229.
15. Knauer, B. R.; Napier, J. J. *J. Am. Chem. Soc.* **1976,** *98*, 4395 – 4400.
16. Janzen, E. G. ; Coulter, G. A.; Oehler, U. M.; Bergsma, J. P. *Can. J. Chem.* **1982**, *60*, 2725–2733.
17. Reichardt, C.; Welton, T. *Solvent and Solvent Effect in Organic Chemistry*, 4th ed., Wiley-VCH, Weinheim, 2011.
18. Marcus, Y. *The Properties of Solvents*, Vol. 4, Wiley, Chichester, 1998.
19. The occurrence of this interaction, and consequently the magnitude of the hcc, depends both on the spin population on the nitrogen atom r_N^P and on the dihedral angle q between the C—P bond and the Singly Occupied Molecular Orbital SOMO (Scheme 1) on the nitrogen atom of the nitroxyl moiety. r_N^P□, the spin population on the nitrogen atom of the nitroxyl moiety, is proportional to a_N. B_0 is the transfer of the spin population through the spin polarization process and B_1 is the transfer of the spin population through the hyperconjugation process. In general, B_0 is very small and can be neglected [16]. Values of B_1 are dependent on the atom or on the function at position b [13,16].